Robotica (2015) volume 33, pp. 2083–2099. © Cambridge University Press 2014
doi:10.1017/S0263574714001301

Dynamic balance optimization in biped robots: Physical modeling, implementation and tests using an innovative formula

G. G. Muscolo[1,2*] , C. T. Recchiuto[3] and R. Molfino[2]

[1]*Creative and Visionary Design Laboratory, Humanot s.r.l., Via Amedeo Modigliani, 7, 59100, Prato, Italy*
[2]*PMAR Lab., DIME-MEC, Scuola Politecnica, University of Genova, Via all'Opera Pia, 15, Genova, Italy*
[3]*Electro-Informatic Laboratory, Humanot s.r.l., Via Amedeo Modigliani, 7, 59100, Prato, Italy*

(Accepted April 7, 2014. First published online: May 22, 2014)

SUMMARY
In this paper, an analytical formula[1] for the determination of the center of mass position in humanoid platforms is proposed and tested in a real humanoid robot. The formula uses the force-torque values obtained by the two force-torque sensors applied on the feet of the robot and the measured currents required from the motors to maintain balance as inputs. The proposed formula outputs the real center of mass position that minimizes the errors between real humanoid robots and virtual models. Data related to the Zero Moment Point positions and to the joint movements are compared with the target values, showing how the application of the proposed formula enables achieving better repeatability and predictability of the static and dynamic robot behaviour.

KEYWORDS: CoM; Posture control; Humanoid robots; Locomotion; ZMP; Mass error.

1. Introduction

Humanoid robots are complex machines built for different purposes (medical research, services, education, entertainment, etc.). During the construction and the maintenance of any humanoid platform, errors normally arise, which separate biped robots from their virtual models (CAD and digital mock-up). These errors can be due to several reasons such as the length of the links, the position of the joints, construction tolerances, etc. . ., and cannot be eliminated.[1] Hence, the real Center of Mass (CoM) of the robot is not coincident with the CoM of its virtual model.[2]

Designers and Robot Manufacturers often give inertial parameter values obtained using CAD software, and do not take into account the mass of cables and wires of the whole actuators and sensors that can be added in a second moment. This can generate inordinate errors in simulated data and in control stability.

Many research groups have tried to overcome this problem using different strategies. Some researchers and specialists in the humanoid robotics field use a "Posture controller",[1,2] in order to reduce the error between the robotic platform and its virtual model. However, the complexity of the whole system increases using a real-time posture controller. The posture controller is often in conflict with the "motion controller" of the robot.[2] Internal conflicts between the two controllers have a high impact on the CPU power and on the controller complexity. In such approaches, the robot converges in a stable posture (for example in a straight position) in a longer time and therefore it cannot be robust and reactive. Furthermore, errors remain between the CoM of the platform and the CoM of its virtual model. Kwon *et al.*[3] proposed a method that uses a closed-loop observer based on a Kalman filter, adopted as estimation framework. Also in this case, the strategy is not aimed

* Corresponding author. E-mail: g.muscolo@humanot.it; muscolo@dimec.unige.it
[1] Italian Patent Pending[10].

at better estimating the center of mass, but at controlling the robot taking into account the possible errors. Ayusawa *et al.*[4] proposed a method based on regression analysis models in order to estimate inertial parameters using a minimal set of sensor. The approach is similar to the one presented in this paper but it is based on an estimation of inertial parameters of a very small robot where the inertial influences have small values. In the work of Sujan and Dubowsky,[5] the dynamic parameters of a mobile robot are calculated using an algorithm based on a mutual-information-based theoretic metric for the excitation of vehicle dynamics. Liu *et al.*,[6] Khalil *et al.*[7] and Swevers *et al.*[8] show other methods oriented to improve the balancing performances of mobile biped robots when the center of mass is not precisely known. However, all these approaches do not deal with the problem of the determination of the effective position of the centre of mass.

In this paper, the authors propose a novel approach to determine the correct position of the center of mass in humanoid robots. In order to compensate the errors between the biped platform and its virtual model, an additional mass has been implemented in the virtual model of the humanoid robot. The value of this mass error is the analytical difference between the weight of the robot and the weight of its virtual model. Its position in the space is not known *a priori*, but it will be approximately calculated with the procedure described in this paper. In order to define its position, the authors of the paper propose an analytic formula, that gives the real position of the CoM of the platform and is based on the application of a procedure that requires only the values of the force-torque sensors, applied on the feet of the humanoid robot, and the values of the motors torque. This procedure standardizes the calibration procedure in order to minimize the errors and it can be applied to every biped platform. In this work, the approach will be applied to a humanoid robot with dimensions comparable to humans (height : 1500 mm; weight: 64 kg). A winning feature is its easy application and industrialization. Some of the benefits obtained using this formula are the improved accuracy in the execution of tasks and the reduction of the errors between the real platform and its virtual model.

This paper begins with the description in details of the proposed formula, presented in its initial formulation in precedent works.[9,10] Next, the robotic platform SABIAN[11] and the virtual models used for the validation of the formula are presented. In the last section, the results of its implementation and the planned next works are discussed.

2. The Proposed Formula

2.1. Center of Mass (CoM) and Error Mass (EM)

A first intuitive step to calibrate a robot is to obtain the highest correlation value between the CoM position of the robot and the CoM position of its virtual model. Theoretically, the two CoMs (real and virtual) should be in the same position but a gap error is actually present between the two CoM positions. In this paper, in order to simplify the problem, we considered all the errors related to the robot concentrated in a mass called "error mass" (EM). The value of this EM is obtained from the difference between the weight of the platform and the weight of the robot in the CAD model. The position in space of the EM is not known and a manual and iterative procedure must be used in order to evaluate it. In general, the manual procedure starts setting the Z position of the EM in the virtual model and determining the X and Y positions, in order to reduce the errors between the trajectories of the ZMP (acronym for Zero Moment Point[12]) generated off-line using the virtual model and measured on-line from the humanoid robot.[13]

The steps performed in a manual and iterative procedure are the following:

1. Build a virtual model of the robot with an additional EM in a fixed Z position and generic X and Y positions, schedule a task for the model, start the virtual simulation and extract data related to the virtual ZMP;
2. Use the virtual ZMP as input on the real platform and extract data related to the real ZMP;
3. Compare the real ZMP and the simulated ZMP.

This procedure continues repeating steps 1) and 2) and changing a teach loop the X and Y positions of the EM in the virtual model until the error between the real and virtual ZMP trajectory goes under an arbitrary threshold. Please note that modifying the position of the EM in the virtual model, the response of the virtual and of the real ZMP changes. Thus, manually finding the correct position of the EM is a very complex process. Another problem is that the manual method is not accurate at all,

https://doi.org/10.1017/S0263574714001301 Published online by Cambridge University Press

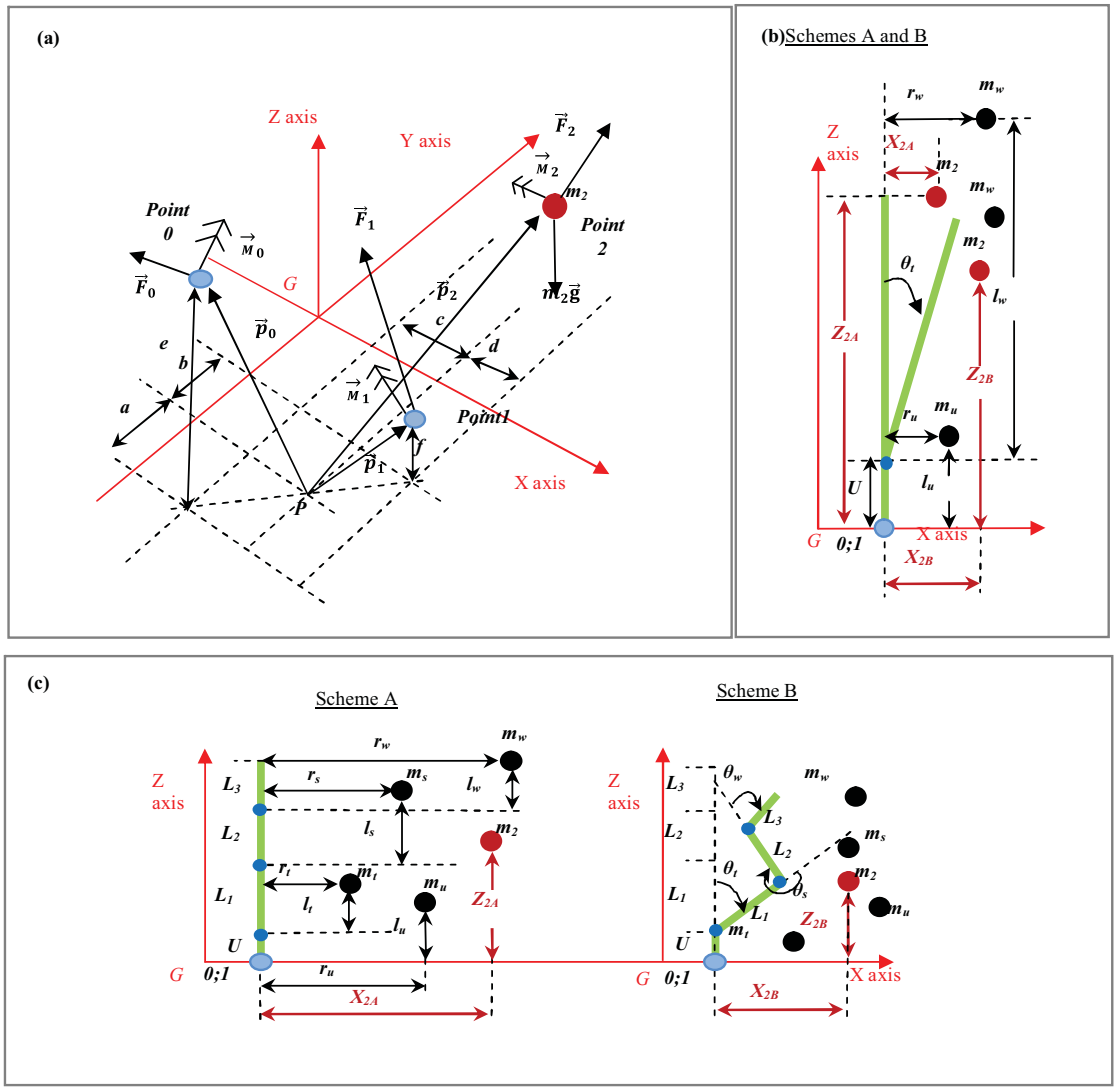

Fig. 1. (a) Scheme used for the definition of the method. The direction of the force and torque vectors is only indicative; (b) two balance configurations (schemes *A* ($\theta_t = 0°$) and *B* ($\theta_t \neq 0°$)); (c) two alternative balance configurations (schemes *A* ($\theta_t = 0°, \theta_w = 0°, \theta_s = 360°$) and *B* ($\theta_t \neq 0°; \theta_s \neq 360°; \theta_w \neq 0°$)). The humanoid robot is shown in green and the joints (or motors) are indicated with blue points. The points 0 and 1 that represent the feet, where the force/torque sensors are positioned, are shown with a light blue colour; the center of mass represented with the point 2 is shown in red; the other black points indicate the mass of the links of the robot.

and therefore it must be frequently repeated. In addition, the Z position of the EM is arbitrary fixed in advance by the user and it can be very far from the real one.

2.2. *Definition of the system*

In this paper we propose an analytical formula in order to determine the real CoM position and consequently the EM position. In the Fig. 1(a), a reference Cartesian system (*G-XYZ*) and three points in the space (*0, 1 and 2*) are shown. The three points can be considered belonging to a rigid body in the space; furthermore, the rigid body can be compared to a humanoid platform, or robot, with its center of gravity in the point 2 and its feet in the points 0 and 1. A humanoid robot is indeed composed of a trunk and articulated kinematic chains such as legs and arms, connected to the trunk with joints and motors, and with force-torque sensors positioned on the feet and on the hands. Figures 1(b) and (c) show a sketch of a humanoid robot in green, while the joints (or motors) are indicated with blue points. The points 0 and 1 that represent the feet, where the force/torque sensors

https://doi.org/10.1017/S0263574714001301 Published online by Cambridge University Press

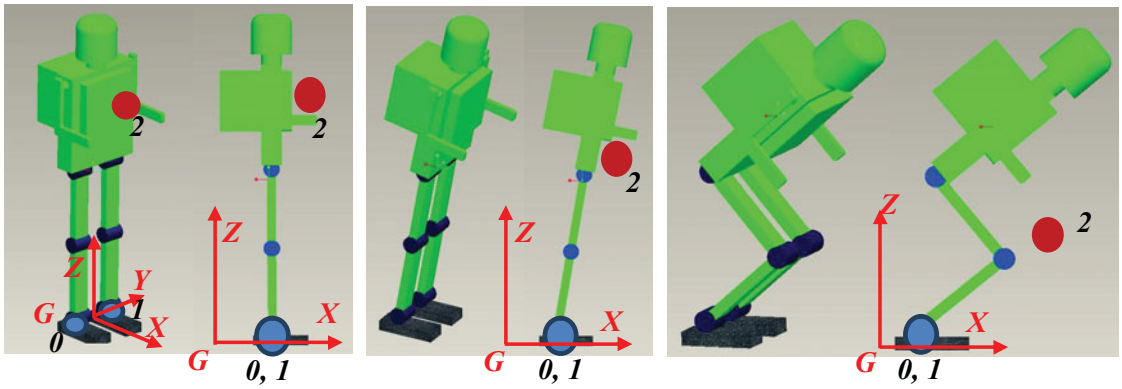

Fig. 2. Schemes used for the definition of the method proposed in the Fig. 1: (a) scheme or configuration A; (b) scheme or configuration B; (c) alternative scheme or configuration B. The meaning of the colours is the same of the Fig. 1.

are positioned, are shown with a light blue colour; the center of mass represented with the point 2 is shown in red; the other black points indicate the mass of the links of the robot. Figure 2 shows a humanoid robot in the same configurations of the schemes A and B of Figs. 1(b) and (c).

The dynamics of the system constituted of the three points (0, 1 and 2) is described by the two following equations (see Fig. 1(a)):

$$m_2 \cdot \vec{a}_2 = m_2 \cdot \vec{g} + \vec{F}_0 + \vec{F}_1 + \vec{F}_2, \tag{1}$$

$$\vec{M}_P = \vec{M}_0 + \vec{M}_2 + \vec{M}_1 + \vec{p}_0 \times \vec{F}_0 + \vec{p}_1 \times \vec{F}_1 + \vec{p}_2 \times \vec{F}_2, \tag{2}$$

where: $\vec{a}_2 = [a_{X2}, a_{Y2}, a_{Z2}]^T$ is the acceleration of the CoM; m_2 is the total mass of the robot without feet; $\vec{p}_0 = [-c, -a, e]^T$ and $\vec{p}_1 = [d, b, f]^T$ are the position vectors shown in Fig. 1(a). $\vec{p}_2 = [X_2, Y_2, Z_2]^T$ is the COM position that will be determined with the proposed formula in this paper. $\vec{M}_0 = [M_{X0}, M_{Y0}, M_{Z0}]^T$, $\vec{M}_1 = [M_{X1}, M_{Y1}, M_{Z1}]^T$, $\vec{M}_2 = [M_{X2}, M_{Y2}, M_{Z2}]^T$, $\vec{F}_0 = [F_{X0}, F_{Y0}, F_{Z0}]^T$, $\vec{F}_1 = [F_{X1}, F_{Y1}, F_{Z1}]^T$, $\vec{F}_2 = [F_{X2}, F_{Y2}, F_{Z2}]^T$ respectively represent the torques ($\vec{M}_0$, $\vec{M}_1$, $\vec{M}_2$) and the forces ($\vec{F}_0$, $\vec{F}_1$, $\vec{F}_2$) aging at the points 0, 1 and 2. $\vec{M}_P = [M_{XP}, M_{YP}, M_{ZP}]^T$ is the resultant moment calculated with respect to the point P (see Fig. 1(a)). The direction of the force and torque vectors, shown in Fig. 1(a), is only indicative; the positive direction of the force and torque vectors has been considered with the same positive direction of the reference Cartesian system (*G-XYZ*).

Furthermore we can say that:

$$\vec{M}_2 = \begin{bmatrix} M_{X2} \\ M_{Y2} \\ M_{Z2} \end{bmatrix} = \begin{bmatrix} \sum M_{j\_\text{roll}} \\ \sum M_{j\_\text{pitch}} \\ \sum M_{j\_\text{yaw}} \end{bmatrix}, \tag{3}$$

M_2 includes only the internal torques; M_0 and M_1 include the ground reaction torques. The Equation (3) is based on the assumption that the Jacobian Matrix is equal to the identity Matrix. This assumption is correct if the joints axis of the robot remain parallel, during motion, to the Y axis of the reference Cartesian system (*G-XYZ*) (see Fig. 2). It means that the motion of the robot for the determination of the formula is performed in a 2D plane. In this paper the XZ plane is considered. $\sum_{j\_\text{roll}}^{M}$, $\sum_{j\_\text{pitch}}^{M}$, $\sum_{j\_\text{yaw}}^{M}$ are the torques of all roll, pitch and yaw motors of the robot[9] and M_j is obtained from the equation:

$$M_j\,[Nm] = K\,[Nm/A] \cdot I\,[A]\,, \tag{4}$$

https://doi.org/10.1017/S0263574714001301 Published online by Cambridge University Press

The accuracy in the estimation of M_j, calculated in (4) depends on the accuracy of the K value that is a constant parameter set for each motor and on the accuracy of the current I necessary for the motor function. In particular, the resolution of the used A/D converters is a fundamental parameter to define the accuracy of the current I.

2.3. Simplification of the system

Considering the robot equilibrium ($m_2\vec{a}_2 = 0; \vec{M}_P = 0$) with respect to the point P as shown in the Fig. 1(a), Eqs. (1) and (2) can be modified. Moving the point of view from the vector shape to the scalar one, the values of the three components x, y and z of the force and the torque can be obtained. The new system consists of six equations (five linearly independent) in six unknown values F_{X2}, F_{Y2}, F_{Z2}, X_2, Y_2, Z_2. The forces and torques in the points 0 and 1 can be calculated by means of the load cells. The torques M_{X2}, M_{Y2}, M_{Z2} are determined using (3) and (4).

In order to simplify the system, the robot is positioned in two different configurations. The two configurations are chosen in order to have a simplified geometry using $a = b$, $c = d = e = f = 0$ (see Figs. 1(a), 1(b), 2(a) and (b)) obtaining $\vec{p}_0 = [0, -a, 0]^T$ and $\vec{p}_1 = [0, a, 0]^T$.

In the first step the robot is placed on a walking surface and the platform should be kept in a first balance configuration (Figs. 1(b) and 2(a) - Scheme A), allowing a measurement of the forces ($\vec{F}_0$, $\vec{F}_1$) and the torques ($\vec{M}_0$, $\vec{M}_1$) by means of the force-torque sensors on the feet, and of the armature currents ($\sum_{j\_\text{roll}}^{M}$, $\sum_{j\_\text{pitch}}^{M}$, $\sum_{j\_\text{yaw}}^{M}$). In a second step, the robot is placed in a second balance configuration (Figs. 1(b) and 2(b) - Scheme B), and in the same way, forces, torques and motor currents associated with this new balance configuration are measured. Figures 1(b), 2(a) and (b) show the two balance configurations in the XZ plane. In particular, the coordinates X_{2A} and Z_{2A} are relative to the position of the center of mass of the platform in the configuration A (Figures 1(b) and 2(a)) along the first straight common line, which is chosen orthogonal to the plane of standing, and then parallel to the Z axis. m_u, r_u, l_u, are the mass and the position of the center of mass of the robot ankle link from the floor to the ankle joint. m_w, r_w, l_w, are the mass and the position of the center of mass of the remaining links of the platform. In the second balance configuration B (Figures 1(b) and 2(b)), the components of the body are aligned according to a second straight common line, inclined to the vertical line with an angle θ_t. While m_u, m_w, r_u, l_u remain constant, r_w and l_w change their values. In this case, X_{2B} and Z_{2B} identify the coordinates of the center of mass of the body in the second balance configuration B. The coordinates of the two feet are the same because we chose this configuration as input. The implementations have been done positioning the robot in this initial position using a leveller and the encoders of the motors.

Based on the choice $a = b$, $c = d = e = f = 0$ ($\vec{p}_0 = [0, -a, 0]^T$ and $\vec{p}_1 = [0, a, 0]^T$), the Eqs. (1) and (2) can be rewritten in a general form that is function of the balance i configuration ($i = A$ or $i = B$). Thus, equations from (5) to (9) are obtained.

$$F_{X2i} = -F_{X0i} - F_{X1i}, \tag{5}$$

$$F_{Y2i} = -F_{Y0i} - F_{Y1i}, \tag{6}$$

$$F_{Z2i} = m_2 \cdot g - F_{Z0i} - F_{Z1i}, \tag{7}$$

$$X_{2i} = -\left(M_{Y0i} + M_{Y1i} + M_{Y2i}\right) / \left(F_{Z0i} + F_{Z1i}\right) + \left[\left(F_{X0i} + F_{X1i}\right) / \left(F_{Z0i} + F_{Z1i}\right)\right] \cdot Z_{2i} \tag{8}$$

$$Y_{2i} = \left[\left(M_{X0i} + M_{X1i} + M_{X2i}\right) / \left(F_{Z0i} + F_{Z1i}\right)\right] + \left[a \cdot \left(F_{Z1i} - F_{Z0i}\right) / \left(F_{Z0i} + F_{Z1i}\right)\right] + \left[\left(F_{Y0i} + F_{Y1i}\right) / \left(F_{Z0i} + F_{Z1i}\right)\right] \cdot Z_{2i}, \tag{9}$$

The Equations (10)–(13) introduce the coefficients α_i, β_i, γ_i, δ_i, and their relations with the force and torque measurements:

$$-\left(M_{Y0i} + M_{Y1i} + M_{Y2i}\right) / \left(F_{Z0i} + F_{Z1i}\right) = \alpha_i, \tag{10}$$

$$\left(F_{X0i} + F_{X1i}\right) / \left(F_{Z0i} + F_{Z1i}\right) = \beta_i, \tag{11}$$

$$\left(M_{X0i} + M_{X1i} + M_{X2i}\right) / \left(F_{Z0i} + F_{Z1i}\right) + \left[a \cdot \left(F_{Z1i} - F_{Z0i}\right) / \left(F_{Z0i} + F_{Z1i}\right)\right] = \gamma_i, \tag{12}$$

$$\left(F_{Y0i} + F_{Y1i}\right) / \left(F_{Z0i} + F_{Z1i}\right) = \delta_i, \tag{13}$$

https://doi.org/10.1017/S0263574714001301 Published online by Cambridge University Press

Thus, Eqs. (8) and (9) (for $i = A$ or $i = B$) can be rewritten in the following form:

$$X_{2i} = \alpha_i + \beta_i \cdot Z_{2i}, \tag{14}$$

$$Y_{2i} = \gamma_i + \delta_i \cdot Z_{2i}, \tag{15}$$

Still with reference to Fig. 1(b), using the parameters m_u, m_w,r_u, l_u,r_w and l_w, the Eqs. (16) and (17) can be obtained. Thus, the Eqs. (14), (16) and (17) can be seen as a system composed of 6 equations in 6 unknown variables (for $i = A$ and $i = B$) X_{2A}, Z_{2A}, X_{2B}, Z_{2B}, r_w, l_w; the relation between m_w and m_u is given by the Eq. (18). θ_t is fixed by the user ($\theta_t = 0$ in $i = A$), in a way that does not allow to tilt the platform.

$$X_{2i} = [m_u \cdot r_u + m_w \cdot (l_w \cdot \sin\theta_t + r_w \cdot \cos\theta_t)]/m_2, \tag{16}$$

$$Z_{2i} = [m_u \cdot l_u + m_w \cdot (U + l_w \cdot \cos\theta_t - r_w \cdot \sin\theta_t)]/m_2, \tag{17}$$

$$m_w = m_2 - m_u, \tag{18}$$

Solving the equations system constituted by (14), (16) and (17), the positions of the center of mass are calculated in both the configurations A and B (for $i = A$ and $i = B$) of the diagram of Fig. 1(b). It must be underlined that only X as a function of Z has been considered, but the same result can be obtained considering Y as a function of Z.

2.4. The proposed formula

Placing $\theta_t = 0$ (then $i = A$) and substituting (16) and (17) into (14) and placing $\theta_t \neq 0$ (then $i = B$) and substituting (16) and (17) into (14), two different equations will be obtained. Finally, combining these two equations l_w and r_w are obtained.

Placing $\theta_t \neq 0$ (then $i = B$) and rewriting (17) with the latter values given by l_w and r_w, Z_{2B} is obtained. Z_{2B} represents the general position of the height Z of the center of mass for any value of θ_t. Placing $i = B$ in (14) and (15) and substituting the found value of Z_{2B}, the general formula of the position of the center of mass in (19) is given. Considering the equilibrium configuration A ($i = A$) and then θ_t equal to zero, the systems (20) and (21) are obtained.

In particular, considering the system (21), the calculation of the center of mass position is strictly related to the coefficients α_A, β_A, γ_A, δ_A, α_B, β_B, that are numerical values associated with the first and second measurements on the robot. In order to calculate these coefficients, it is necessary to consider the arbitrary θ_t associated with the second balance configuration, in addition to other parameters such as the above mentioned position of the center of mass of the feet (r_u and l_u) and its mass (m_u) calculated using the CAD model. These parameters have a lower weight with respect to other links of the platform and then a lower inertial influence.

$$\begin{cases} Z_{2B} = f\,(\theta_t, m_2, \beta_B, \beta_A, \alpha_A, m_u, l_u, m_w, U, r_u, \alpha_B)\,, \\ X_{2B} = \alpha_B + \beta_B \cdot Z_{2B}, \\ Y_{2B} = \gamma_B + \delta_B \cdot Z_{2B}, \end{cases} \tag{19}$$

$$\begin{cases} Z_{2B}\,(\theta_t = 0) = Z_{2A} = f\,(m_2, \beta_B, \beta_A, \alpha_A, m_u, l_u, m_w, U, r_u, \alpha_B)\,, \\ X_{2B}\,(\theta_t = 0) = X_{2A} = \alpha_A + \beta_A \cdot Z_{2A}, \\ Y_{2B}\,(\theta_t = 0) = Y_{2A} = \gamma_A + \delta_A \cdot Z_{2A}, \end{cases} \tag{20}$$

$$\begin{cases} X_{2A} = (\beta_A \cdot \alpha_B - \alpha_A \cdot \beta_B)\,/\,(\beta_A - \beta_B)\,, \\ Y_{2A} = [\gamma_A \cdot (\beta_A - \beta_B) + \delta_A \cdot (\alpha_B - \alpha_A)]\,/\,(\beta_A - \beta_B)\,, \\ Z_{2A} = (\alpha_B - \alpha_A)\,/\,(\beta_A - \beta_B)\,, \end{cases} \tag{21}$$

Alternatively, the same method can be implemented with a different second balance configuration B, shown in a schematic way in Figs. 1(c) and 2(c).

In this variant, the components of the body are located along a broken line. In the shown example, the body is composed of 4 links and 3 joints. Three angles should be considered: θ_t, as in the Fig. 1(b), a rotation angle θ_s in correspondence of its knees, and θ_w defined by the rotation of his torso with respect to legs.

https://doi.org/10.1017/S0263574714001301 Published online by Cambridge University Press

In this case, the alternative system composed of the Eq. (14), (16') and (17') is obtained. The angle values are obtained considering the Eq. (22).

$$X_{2i} = [m_u \cdot r_u + m_t \cdot (l_t \sin\theta_t + r_t \cos\theta_t) + m_s \cdot (L_1 \sin\theta_t - l_s \sin\theta_r + r_s \cos\theta_r) + m_w \cdot (L_1 \sin\theta_t - L_2 \sin\theta_r) + m_w \cdot (l_w \sin\theta_n + r_w \cos\theta_n)]/m_2, \quad (16')$$

$$Z_{2i} = [m_u \cdot l_u + m_t \cdot (U + l_t \cos\theta_t - r_t \sin\theta_t) + m_s \cdot (U + L_1 \cos\theta_t + r_s \sin\theta_r + l_s \cos\theta_r) + m_w \cdot (U + L_1 \cos\theta_t + L_2 \cos\theta_r) + m_w \cdot (l_w \cos\theta_n - r_w \sin\theta_n)]\frac{1}{m_2}, \quad (17')$$

$$\theta_r = 2\pi - (\theta_t + \theta_s); \quad \theta_n = \theta_w - \theta_r, \quad (22)$$

The unknown parameters are the same as the previous system and the additional values related to the other system are calculated using the CAD model. The angle values $\theta_t, \theta_s, \theta_w$, respectively represent the orientation of the ankle, knee and hip joints of the robot. With the condition of $\theta_t = 0°, \theta_s = 360°, \theta_w = 0°$, the same system (21) is obtained.

Solving the system (21), the position of the effective center of mass of the humanoid platform without feet is given, combining the numerical values associated with the first and second balance configurations A and B.

2.5. Real center of mass position

Using (23), (24) and (25), the parameters relative to the weight and the geometric position of the center of mass of the feet of the platform can be calculated. In this equations m_V, X_V, Y_V, Z_V, are the values of the mass and the center of mass position of the total virtual model of the robot and m_C, X_C, Y_C, Z_C, are the values of the mass and the center of mass position of the virtual model of the robot without feet. In (26), (27) and (28), the position of the effective center of mass of the platform with the feet is indicated with $X_R, Y_R, Z_R.X_F, Y_F, Z_F$, represent the feet positions. The feet have a lower weight with respect to other links of the platform and then a lower inertial influence.

$$X_F = \frac{X_V \cdot m_V - X_C \cdot m_C}{m_V - m_C}, \quad (23)$$

$$Y_F = \frac{Y_V \cdot m_V - Y_C \cdot m_C}{m_V - m_C}, \quad (24)$$

$$Z_F = \frac{Z_V \cdot m_V - Z_C \cdot m_C}{m_V - m_C}, \quad (25)$$

$$X_R = \frac{X_2 \cdot m_2 + X_F \cdot (m_V - m_C)}{m_2 + m_V - m_C}, \quad (26)$$

$$Y_R = \frac{Y_2 \cdot m_2 + Y_F \cdot (m_V - m_C)}{m_2 + m_V - m_C}, \quad (27)$$

$$Z_R = \frac{Z_2 \cdot m_2 + Z_F \cdot (m_V - m_C)}{m_2 + m_V - m_C}, \quad (28)$$

3. Humanoid Platform and Virtual Models

3.1. Humanoid robot

The humanoid robot SABIAN (Fig. 3(a)) (Table I)[11] is obtained assembling two different parts of widely known humanoid robots: WABIAN 2-R[13,14] (trunk and legs) and ICUB[15] (head). Some differences between WABIAN 2R and SABIAN can be underlined.[11,16]

https://doi.org/10.1017/S0263574714001301 Published online by Cambridge University Press

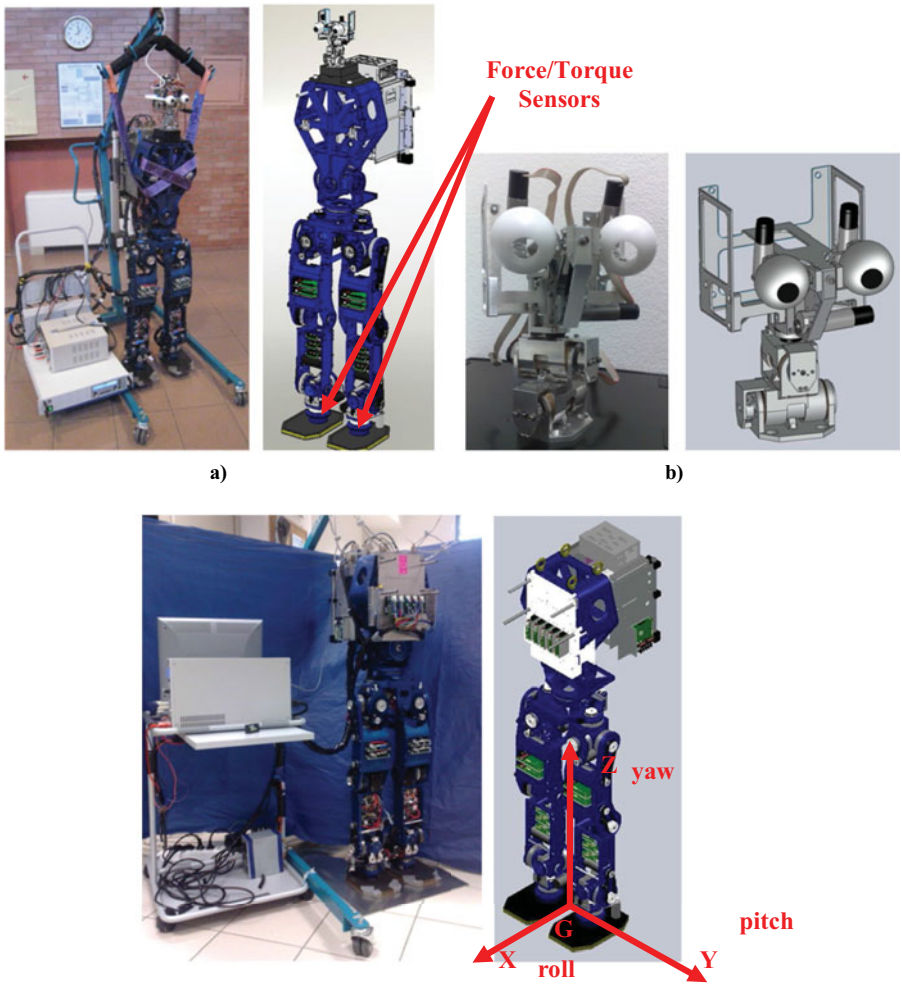

Fig. 3. (a) SABIAN (real picture and CAD model); (b) SABIAN head, copy of the ICUB robot; (c) SABIAN without head used for tests (courtesy of the Scuola Superiore Sant'Anna).

In this paper the authors used the platform of the Fig. 3(c) for the validation tests of the formula and the physical simulator of the Fig. 4 to construct the virtual models of the robot.

The electronic hardware dedicated to the motion control of the SABIAN is mounted on the trunk and consists of a PCI CPU board and two PCI I/O boards. As I/O boards, a HRP interface board (16ch D/As, 16ch counters, 16ch PIOs) and a 6-axis force/torque sensor receiver board are mounted. The operating system is QNX Neutrino ver. 6.3. The drive system consists of a DC servo motor with an incremental encoder attached to the motor shaft and a photo sensor to detect the basing angle. Furthermore, each ankle has a 6-axis force/torque sensor, used to measure Ground Reaction Force (GRF) and Zero Moment Point (ZMP).

3.2. Robot control system

The walking control system of the SABIAN has two execution phases.[11] The first phase uses a pattern generator that calculates the trajectory of the end-effectors (represented by the feet). Then, the trajectories to be executed are sent to the robot. The SABIAN Pattern Generator uses the feet positions file in order to create the motion pattern of the lower limbs. Additionally, for the dynamic balance of the humanoid robot during the walking stages, legs and waist motions are corrected by a walking stabilization control (Motion Control) that is based on the ZMP position. In this way we have an ideal motion pattern, and a real one with the online corrections due to the control.

https://doi.org/10.1017/S0263574714001301 Published online by Cambridge University Press

Table I. SABIAN characteristics (courtesy of the Scuola Superiore Sant'Anna).

Characteristics	SABIAN without head used for tests (see Fig. 3(c))
Height [mm]	1300
Weight [kg]	40,75
DOF	Leg 7 × 2 / Foot 0 / Waist 2 / Trunk 2 (not working) / Arm 0 / Hand 0 / Neck 0. Total: 16.
Sensors and Actuators	2 Force/Torque triaxial sensors; Photo-sensors; Magnetic incremental Encoders. Servo Motors DC with Harmonic drive (HD).

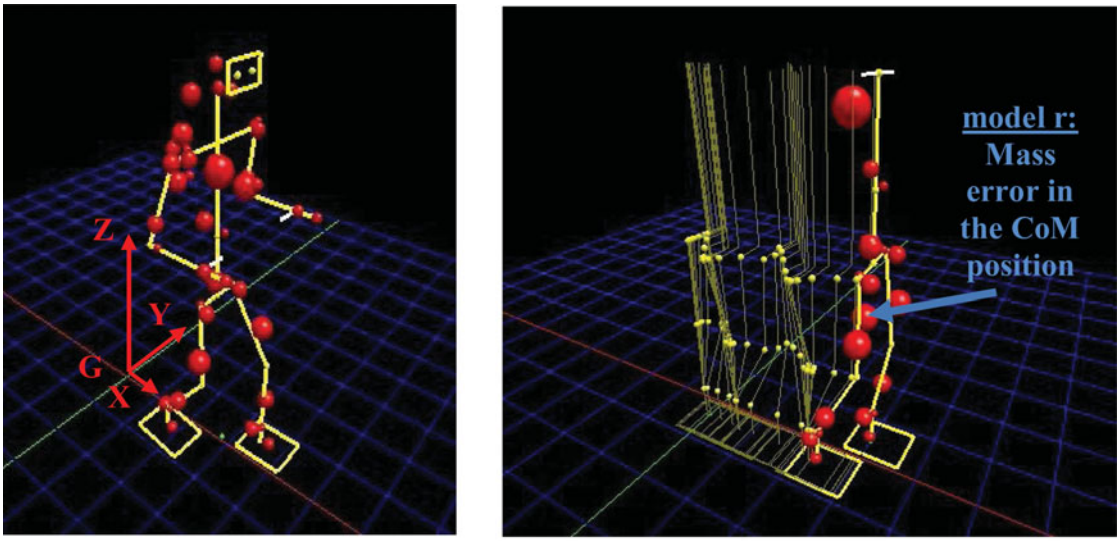

Fig. 4. GUI of the used Pattern Generator to construct virtual models: (a) complete virtual humanoid robot with masses (red balls) of each link; (b) virtual SABIAN robot with the mass error positioned in the COM calculated with the formula (21) (courtesy of the Scuola Superiore Sant'Anna).

3.3. Robot accuracy and resolution

SABIAN motors provide a voltage signal proportional to the motor output torque through their Servo Driver modules. The resolution of the provided torque monitoring is equal to 0.4% of the maximum motor torque. Between each foot and leg (ankle) of SABIAN a six axis force/torque sensor is present. This sensor can measure a maximum force and torque of 2000 N and 105 Nm, respectively, with an accuracy lower than 1% of the full scale.

There are also two different versions of the Servo Drivers: TD12770-48W 05 and TD12770-48W 10 able to provide respectively 15 and 30 A to the motors, with a maximum voltage of 48V. The drivers have the only task to provide the desired outputs and to provide to the motherboard a voltage signal proportional to the motor torque, but without any low-level control. The motherboard PCI-6881 is connected, with a PCI bus, to a JR3 board for the reading of the six axis force/torque sensors and with 1 HRP interface board to read the encoder signals, the motor torque, the photo sensors, and to give the 16 analog inputs to the servo drivers. The HRP interface boards are equipped with 2 Digital-to-Analog and 2 Analog-to-Digital Converters. In the SABIAN structure only 16 actuated joints are actually present. A detailed description of the SABIAN hardware and software is presented in precedent works.[11,16]

3.4. Virtual models

The method described in the previous paragraphs has been implemented and tested on the SABIAN biped platform. The two balance configurations have been chosen as in Figs. 1(b), 2(a) and 2(b). The effective position of the center of mass (X_R, Y_R, Z_R) of the robot has been calculated by using the formula (21) proposed in the previous section and adding the *x, y, z* positions of the feet located under the load cells (using (26), (27), (28)). In order to test and validate the formula, four virtual models

https://doi.org/10.1017/S0263574714001301 Published online by Cambridge University Press

of the SABIAN humanoid robot have been created considering four different positions of the error mass (EM):

1. the EM positioned in the CoM calculated with the Eqs. (21), (26), (27) and (28) of the proposed formula (X_R, Y_R, Z_R) (*model r*);
2. the EM not considered in the virtual model (*model n*);
3. the EM positioned in a casual position (X_S, Y_S, Z_S) (*model s*). In particular, the EM is positioned near the theoretical position of the head in order to destabilize the system and to obtain the limit values to define the workspace of the EM;
4. the EM positioned in the virtual CoM generated by the CAD model (X_V, Y_V, Z_V) (*model v*).

In the SABIAN platform the measured value of the mass error is 4.622 Kg. This high value of the mass error produces imbalance during walking. The values of the X_R, Y_R, Z_R positions in *mm* are respectively -8, 5.1, 337.3. The values of the X_S, Y_S, Z_S and the X_V, Y_V, Z_V positions in *mm* are respectively 125, 17, 1331.68, -16.38, 0.26, 643.22. All values are calculated with respect to the Cartesian *(G-XYZ)* system shown in Figs. 2(a) and 3(c). The accuracy of the measured currents in (4) is equal to 0.4% and it is related to the A/D converters of the SABIAN robot. Figure 4 shows the GUI of the SABIAN Pattern Generator used to construct the four virtual models. The red balls in the Fig. 4 represent the masses of each link of the robot.

Data related to the difference between the simulated and the real ZMP trajectories will be taken into account to validate the formula. The protocol of the experiments and the discussions of the results are presented in the section below.

4. Experimental Trials and Results

4.1. Experimental setup

A simple gait has been implemented in order to test the behaviour of the robot with the four different models and to demonstrate the effectiveness of the approach. The gait was first designed and simulated with the offline Pattern Generator software[13] (Fig. 4) in order to obtain the feet positions files necessary to perform the walk. The walking process consists of three stages: 128 phases for the start still stage; 256 phases for the actual movement: eight walking steps (right and left alternated) of 300 mm along the X (forward) direction of the global referent system (only the first and the last steps are of 150 mm); 128 phases for the end still stage. Every phase lasts 0.03 seconds, so the experiments were done with a step cycle of 0.96 s/step. Walking experiments were carried out on a horizontal flat plane and five runs were performed with each of the four models. In this walking process the tip of the toe and the heel of the biped robot contact to the ground at the same time.

4.2. Results

During the motion, data related to the effective joints and ZMP positions were collected, stored and compared to the virtual (target) ones. The online Motion Control[13,14] is used to correct any error between the ideal modelling and real data. The correlation between ideal and effective ZMP and the Root Mean Square (RMS) of the difference of these signals were calculated. The temporal traces of the ZMP Y position, calculated with respect to the waist of the robot and for each of the four models is shown in the Fig. 5, where the target position and the real ones are overlapped. In all presented data of this paper, a mean value among the five runs has been considered.

Same considerations about correlation values and RMS errors were assessed for the ideal and real ZMP in the XY Plane (correlation between ideal and real distance from the origin and RMS of the signals).

Figures 6–8 show the absolute ZMP position in the XY plane and the error between ideal and real values.

In addition to the simple position, velocity and acceleration data (ideal values in relation with the real values) have been also considered by differentiating collected and target position data. Finally, the errors and correlations among ideal and effective positions, velocity and accelerations of the 16 joints were assessed.

Data related to the roll and pitch joints related to one of the legs of the robot are shown. All results are summarized in Tables II–IV (best data for every line are highlighted in bold), while the Fig. 9

https://doi.org/10.1017/S0263574714001301 Published online by Cambridge University Press

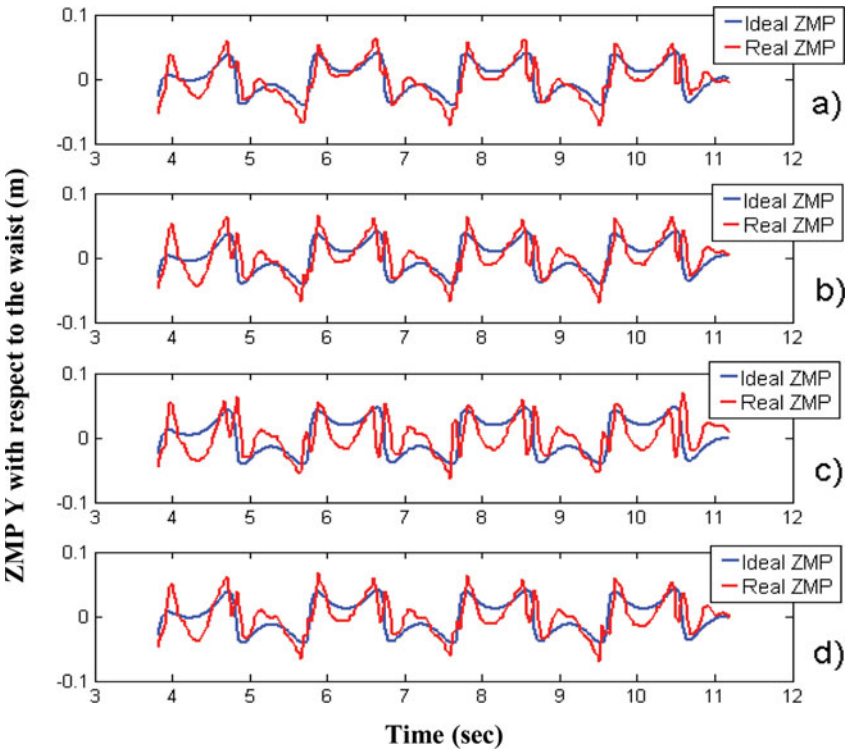

Fig. 5. Ideal and Real ZMP Y position obtained with the models r (a), n (b), s (c), v (d). The graphs are relative to the waist trajectory.

Table II. Correlation data between ideal and real values (ZMP trajectory).

Type of data	Model r	Model n	Model s	Model v
X pos. [m]	**0.8709**	0.8418	0.7370	0.8357
Y pos. [m]	**0.7799**	0.6959	0.4432	0.6710
XY pos. [m]	**0.7337**	0.7073	0.5748	0.6768
X vel. [m/s]	**0.5212**	0.4389	0.2401	0.4293
Y vel. [m/s]	**0.4118**	0.3069	0.1306	0.2992
XY vel. [m/s]	**0.5232**	0.4950	0.4639	0.4910

shows the overlapping between the real and the target positions related to the roll joint of the hip of the model r. Data will be discussed in the next chapter.

5. Discussions

5.1. Analysis of numerical values

The Table II shows the correlation data related to the ideal and real ZMP position and the velocity trajectories.

As can be seen, using the model r, the effective position and velocity of the ZMP X, Y and XY resulting from the walking experiments are more correlated to the target ZMP position and velocity. This means that the resulting walking pattern is more repeatable and predictable consideringthe mass configuration calculated with the proposed method than with other reasonable mass models. A similar consideration can be done by looking at Table III, in which the RMS error value between the real position, velocity and acceleration of the ZMP X, Y and XY are presented for all the four mass models; in almost all cases, the ZMP error value is lowest with mass model r.

Data related to the joint movements are also taken into account. The virtual target positions, velocities and accelerations of the ankle and hip joints of one of the SABIAN legs (data related to the

https://doi.org/10.1017/S0263574714001301 Published online by Cambridge University Press

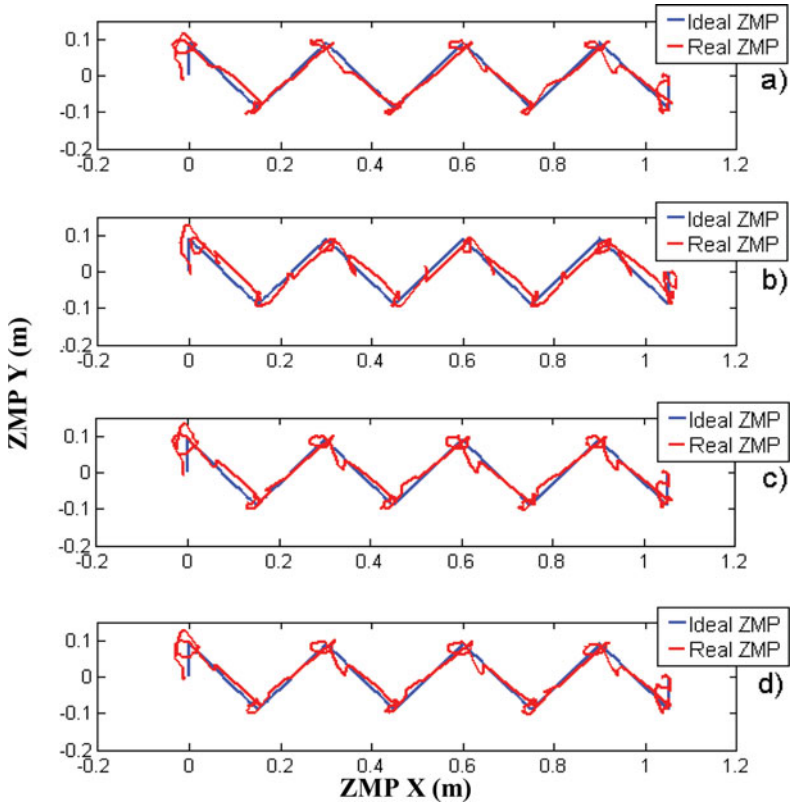

Fig. 6. Ideal and Real absolute ZMP XY position obtained with the models r (a), n (b), s (c), v (d).

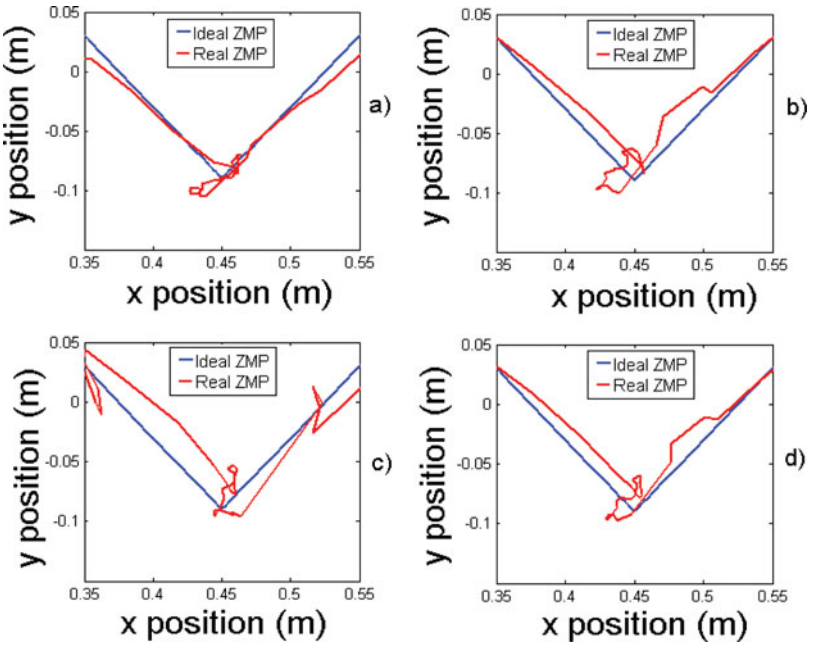

Fig. 7. Ideal and Real absolute ZMP XY position obtained with the models r (a), n (b), s (c), v (d) around a foot-ground contact point.

https://doi.org/10.1017/S0263574714001301 Published online by Cambridge University Press

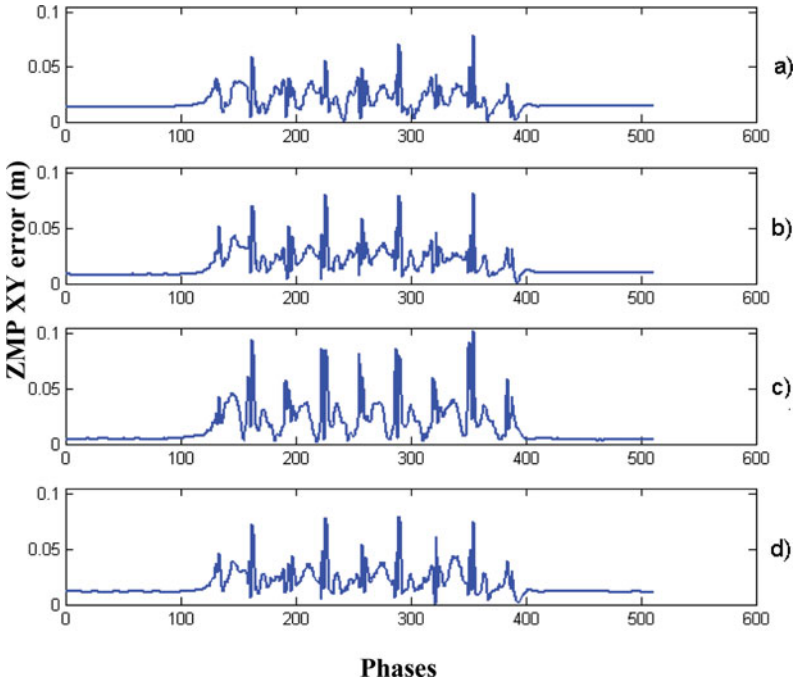

Fig. 8. Error between Ideal and Real ZMP XY position obtained with the models r (a), n (b), s (c), v (d).

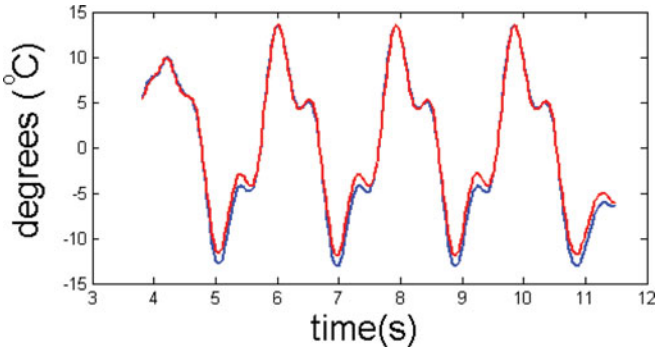

Fig. 9. Ideal and Real hip roll joint positions obtained with the model r.

other leg are similar) have been compared with the effective positions, velocities and accelerations measured during the walking phases. The peak-to-peak error data between virtual and real terms are shown in the Table IV. It can be easily seen that the model r gives the best performances in terms of error (peak-to peak error) between the target joints movement and the real one. This is particularly true for the target accelerations, in which the difference between the adoption of the proposed method and the usage of other empiric methodologies is more evident. It can be also underlined that the method works particularly well for the roll joints, where positions, velocities and accelerations always show a lower error (respect to the target) using the model r than with the other models.

5.2. Analysis of graphs

Figures 5–9, shown in this paper, confirm that using model r is the best choice. Figures 5 and 6 showthat the gap error between the real and virtual value is reduced using the formula (21) proposed in this paper. In the contact point between the robot foot and the ground, represented in the Fig. 7, the model r allows to overlap the virtual trajectory with a higher resolution respect to the other considered models. The reader should note that this is a critical point where the direction of the motion of the robot changes. Figure 8 confirms the goodness of the proposed formula (21): the error committed by

https://doi.org/10.1017/S0263574714001301 Published online by Cambridge University Press

Table III. RMS data between ideal and real values (ZMP trajectory).

Type of data	Model r	Model n	Model s	Model v
X pos. [m]	0.0179	0.0164	**0.0142**	0.0171
Y pos. [m]	**0.0142**	0.0161	0.0224	0.0169
XY pos. [m]	**0.0229**	0.0230	0.0265	0.0240
X vel. [m/s]	**0.2611**	0.2885	0.3369	0.2866
Y vel. [m/s]	**0.3651**	0.4228	0.5070	0.4181
XY vel. [m/s]	**0.4492**	0.5199	0.6088	0.5071
X acc. [m/s^2]	**11.2278**	12.5505	14.0172	12.4586
Y acc. [m/s^2]	**15.7074**	17.8598	19.8534	17.8414
XY acc. [m/s^2]	**19.3339**	21.8301	24.3073	21.7749

Table IV. Peak-to-peak error data (ankle and hip joints of one of the SABIAN legs).

Type of data		Model r	Model n	Model s	Model v
Ankle	pos. [m]	**0.9152**	0.9503	1.4029	0.9601
Roll	vel. [m/s]	**13.0001**	14.2516	17.4744	14.0002
	acc. [m/s^2]	**408.718**	476.992	470.902	470.478
Ankle	pos. [m]	1.0335	1.0124	**0.8262**	0.9887
Pitch	vel. [m/s]	**9.722**	10.070	12.696	9.749
	acc. [m/s^2]	**284.587**	322.524	363.347	316.006
Hip	pos. [m]	0.8057	**0.7700**	0.7898	0.8290
Pitch	vel. [m/s]	**9.5832**	10.7986	13.1327	10.4683
	acc. [m/s^2]	**285.229**	313.548	366.020	307.885
Hip	pos. [m]	**2.1182**	2.1509	2.8876	2.2097
Roll	vel. [m/s]	**24.635**	27.642	33.800	27.455
	acc. [m/s^2]	**660.919**	774.205	891.717	729.873

the pattern generator using the model r is lower with respect to the errors noted using other virtual models. The Figure 9 shows the results described in the Table IV.

5.3. Other considerations

It must be also underlined that the considered model is not exactly the one that perfectly fit the real mass distribution; in this case, the mass error was placed in the Center of Mass (CoM). The best way to obtain a solution that is closer to the effective mass configuration would be to calculate a EM for each link, and add them to the model. Future works will go further in this direction. Another interesting point is that in most of the analysed data, the second best mass configuration was *n*, which has the theoretical structure without any mass error. Thus, it could be underlined that for a simple forward walk, the absence of any mass error can give better results than using a wrong EM. The authors think that this is a very interesting point in the field of the biped locomotion research.

6. Application of the Proposed Formula

Figure 10 shows that on the SABIAN, maximum and the minimum absolute ZMP Y values are about 120 mm and -100 mm, using its online pattern generator[13,14] and implementing the formula (21) proposed in this paper, while without using the formula (21) values were about 150 mm and -110 mm.

The measured maximum and minimum absolute ZMP Y values obtained using the sameonline pattern generator[13,14] described in this paperon the robot WABIAN-RIV were respectively about 160 mm and -170 mm[13] (see Fig. 11) and using the last version of the pattern the maximum and minimum absolute ZMP Y values were respectively 240 mm and -240 mm.

In Kagami *et al.*[17] the authors describe a method that, using a very interesting algorithm, makes the real trajectory converge to overlap the ideal one. Figure 12 shows the ZMP X and ZMP Y on

https://doi.org/10.1017/S0263574714001301 Published online by Cambridge University Press

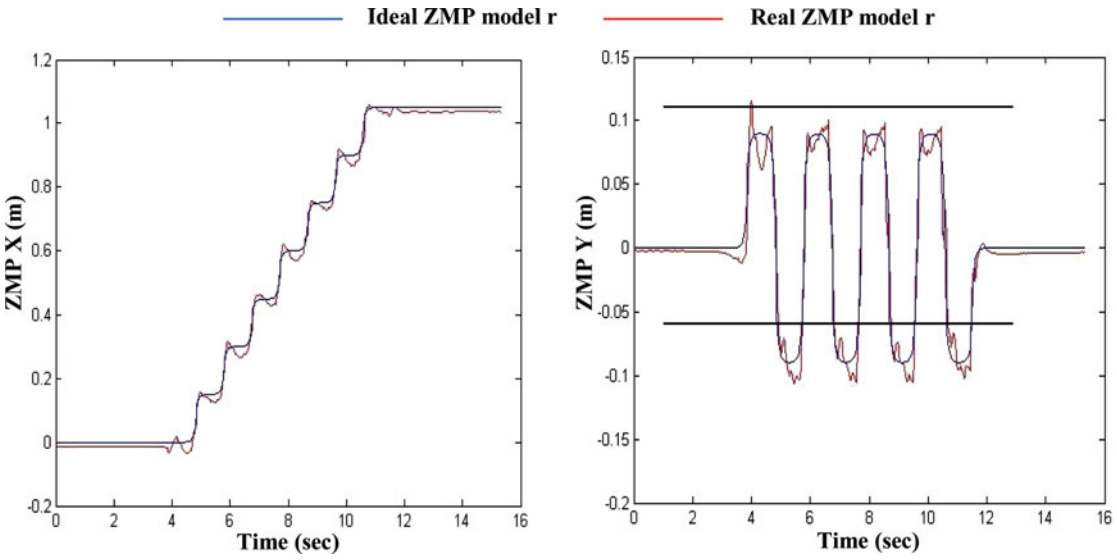

Fig. 10. Absolute ZMP X and Y of the model r proposed in this paper using the formula (21).

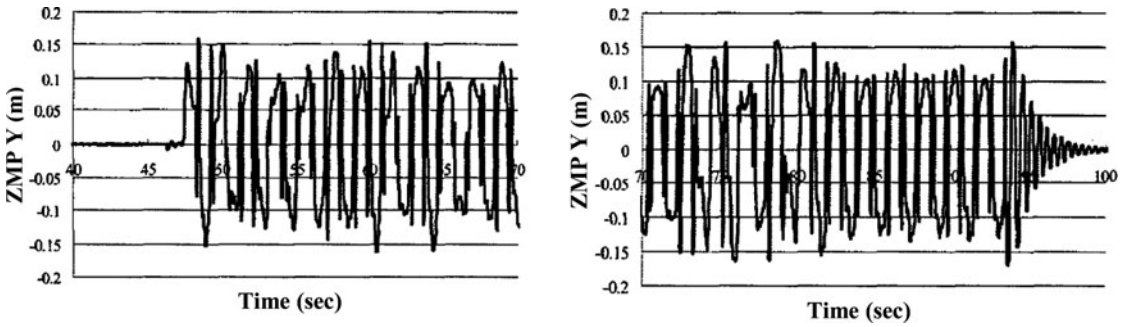

Fig. 11. Absolute ZMP Y of the method proposed by Lim *et al.*[13]

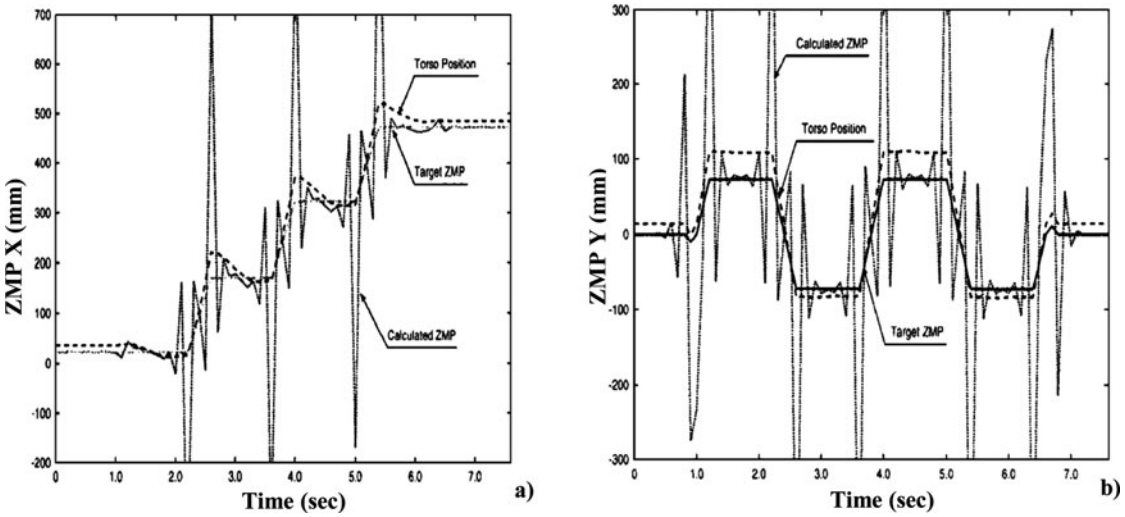

Fig. 12. Absolute ZMP X (a) and Y (b) of the platform usedby Kagami *et al.*[17] before using his proposed method.

https://doi.org/10.1017/S0263574714001301 Published online by Cambridge University Press

the platform used by Kagami *et al.* before applying the algorithm proposed in their paper. Theirwork also underlines that errors are presents in every robotic platform.

In particular, the calculated ZMP X (see Fig. 12(a)) oscillates between 700 mm and −200 mm and the calculated ZMP Y (see Fig. 12(b)) oscillates between 300 mm and -300 mm. The formula (21) can be used to calibrate the platform used by Kagami *et al.* before using the algorithm proposed in their paper, making the convergence from the real trajectory to the ideal one faster and minimizing deviations. An error will always be present, even in a more accurate humanoid robot, such as the HRP-2 prototype;[18] it could be reduced using the formula (21).

The implementation of the proposed formula is also recommended in compliant humanoid robots such as the robot presented by Vanderborght,[19] where the ZMP X seems to have bigger values.

7. Conclusions

In this paper, a new method for the determination of the position of the CoMis proposed. The developed methodology can be applied to any humanoid robot.

The formulation was first theoretically explained and then tested with a simple walking pattern of eight walking steps using the biped humanoid platform SABIAN, in comparison with other reasonable configuration of masses. The aim of the experiment is to demonstrate that the mass configuration resulting from (21) gives the better results in terms of correlation and RMS error between the planned ZMP and the real one; in other words, that the real implementation of the motion pattern is closer to the theoretical one.

The good results shown in this paper create the bases for future works: more analysis with other control systems and different kinds of gaits are planned. Next work will be oriented to improve the calculation of the error mass position of each link of the robot. Additionally, other tests will be performed by means of the WABIAN platform and other humanoid robots and they will be oriented to achieve an optimization of the procedure. However, from the analysis of the shown data, it seems clear that the position of the error mass plays a very important role in the implementation of a stable and repeatable walk. Even though the stability control tries to correct any error arising from differences between the ideal modelling and reality, working with a configuration of masses closer to reality can achieve better results, preventing unwanted oscillations and deviations from the equilibrium position. Thus, this paper offers the possibility to use an analytic formula giving to the final user a very accurate position of the CoM of any humanoid platform using only2 force-torque sensors and motor torque signals without any iterative and manual procedure.

Acknowledgements

The authors would like to acknowledge their friends and colleagues at the Scuola Superiore Sant'Anna and at the Italian Institute of Technology in Pontedera (Pisa, Italy), for their assistance, support, and for the enlightening discussions during the tests performed with the SABIAN robot, in particular Eng. Giacomo Giachetti and Eng. Roberto Lazzarini for their technical support.

The authors would also like to acknowledge their friends and colleagues at the Waseda University (Tokyo, Japan), and they are especially grateful to Dr. Kenji Hashimoto, for his assistance, support, and enlightening discussions. Beside, the authors would also like to show their gratitude to Prof. Paolo Dario, who gave the possibility to collaborate with the Waseda University and with the laboratory of the Prof. Atsuo Takanishi.

References

1. J.-H. Kim, J.-Y. Kim and J.-H. Oh, "Adjustment of Home Posture of Biped Humanoid Robot Using an Inertial Sensor and Force Torque Sensors", *Proceedings of the 2007 IEEE/RSJ InternationalConference on Intelligent Robots and Systems*, San Diego, CA, USA (Oct. 29 – Nov. 2, 2007).
2. V. Nunez, N. Nadjar-Gauthier, K. Yokoi, P. Blazevic and O. Stasse,"Inertial Forces Posture Control for Humanoid Robots Locomotion". *Humanoid Robots: Human-like Machines*, Itech, Vienna, Austria (Jun. 2007) 642 pp.
3. S. J. Kwon and Y. Oh, "Estimation of the Center of Mass of Humanoid Robot", *Proceedings of the International Conference on Control, Automation and Systems 2007*, COEX, Seoul, Korea (Oct. 17–20, 2007).

4. K. Ayusawa, G. Venture and Y. Nakamura, "Identification of Humanoid Robots Dynamics Using Floating-base Motion Dynamics", *Proceedings of the 2008 IEEE/RSJ International Conference on Intelligent Robots and Systems, Acropolis Convention Center*. Nice, France (Sept. 22–26, 2008).
5. V. A. Sujan and S. Dubowsky, "An optimal information method for mobile manipulator dynamic parameter identification," *IEEE/ASME Trans. Mechatronics* **8**(2), 215–225 (Jun. 2003).
6. G. Liu, K. Iagnemma, S. Dubowsky and G. Morel, "A Base Force/Torque Sensor Approach to Robot Manipulator Inertial Parameter Estimation", *Proceedings of the 1998 IEEE International Conference on Robotics & Automation*, Leuven, Belgium, vol. 4 (May 16–20, 1998) pp. 3316–3321.
7. W. Khalil, M. Gautier and P. Lemoine, "Identification of the Payload Inertial Parameters of Industrial Manipulators", *2007 IEEE International Conference on Robotics and Automation*, Roma, Italy (Apr. 10–14, 2007).
8. J. Swevers, C. Ganseman, D. B. Tukel, J. De Schutter and H. Van Brussel, "Optimal robot excitation and identification", *IEEE Trans. Robot. Autom.* **13**(5), 730–740 (Oct. 1997).
9. G. G. Muscolo, C. T. Recchiuto, K. Hashimoto, C. Laschi, P. Dario and A. Takanishi, "A Method for the calculation of the effective Center of Mass of Humanoid robots", available at: http://www.humanoids2011.org/11th IEEE-RAS International Conference on Humanoid Robots, Bled-Slovenia (Oct. 26th - 28th, 2011).
10. G. G. Muscolo and C. T. Recchiuto, "Metodo per il calcolo del centro di massa per una piattaforma umanoide," *Italian Patent Pending. FI2011A000232.* (Oct. 21th, 2011).
11. G. G. Muscolo, C. T. Recchiuto, K. Hashimoto, P. Dario and A. Takanishi, "Towards an Improvement of the SABIAN Humanoid Robot: from Design to Optimization", *J. Mech. Eng. Autom.* **2**(4), 80–84 (2012).
12. M. Vukobratović, "Zero-Moment Point — thirty five years of its life," *Int. J. Humanoid Robot.* **1**(1), 157–173c (2004).
13. H.- Lim, Y. Kaneshima and A. Takanishi,"Online Walking Pattern Generation for Biped Humanoid Robot with Trunk", *Proceedings of the 2002 IEEE International Conference on Robotics & Automation*, Washington, DC (May 2002).
14. H. Lim and A. Takanishi, "Biped walking robots created at Waseda University: WL and WABIAN family". *Phil. Trans. R. Soc.* A, 49–64 365 (2007).
15. R. Beira, M. Lopes, M. Praça, J. Santos-Victor, A. Bernardino, G. Metta, F. Becchi and R. Saltarén, "Design of the Robot-Cub (iCub) Head," *Proceedings of the 2006 IEEE International Conference on Robotics and Automation*, Orlando, Florida (May 2006).
16. G. G. Muscolo, K. Hashimoto, A. Takanishi and P. Dario, "A comparison between two force-position controllers with gravity compensation simulated on a humanoid arm," *J. Robot.*, Hindawi Publishing Corporation (2013).
17. S. Kagami, T. Kitagawa, K. Nishiwaki, T. Sugihara, M. Inaba and H. Inoue, "A fast dynamically equilibrated walking trajectory generation method of humanoid robot," *Auton. Robots* **12**, 71–82 (2002).
18. S. Kajita, F. Kanehiro, K. Kaneko, K. Fujiwara, K. Harada, K. Yokoi and H. Hirukawa, "Biped walking pattern generation by using preview control of zero-moment point," *Proceedings of the 2003 IEEE International Conference on Robotics & Automation*, Taipei, Taiwan (Sep. 14–19, 2003).
19. B. Vanderborght, "Dynamic Stabilisation of the Biped Lucy Powered by Actuators with Controllable Stiffness", Star, Springer tracts in advanced robotics, 63 (2010).

https://doi.org/10.1017/S0263574714001301 Published online by Cambridge University Press